Guidelines for Dryer Design Based on Results from Non-Fickian Model

Madhu Vinjamur, Richard A. Cairncross

Department of Chemical Engineering, Drexel University, Philadelphia, Pennsylvania 19104

Received 4 September 2001; accepted 5 May 2002

ABSTRACT: In polymer solution coatings below the glass transition temperature of the pure polymer, the coating can go undergo a glass transition and develop stresses during drying. When stresses develop, a non-Fickian model accurately describes solvent mass transport in drying polymer coatings. The non-Fickian model includes the solvent transport due to both stress and concentration gradients. This article presents a non-Fickian model, which predicts a lower residual solvent than does the corresponding Fickian model. We showed in an earlier article that the non-Fickian model predicts *trapping skinning* (higher residual solvent under more intense operating conditions) at higher drying gas-flow rates. In this article, the non-Fickian model was used to investigate how the gas-flow rate, dry film thickness, and substrate thickness affect the residual solvent for a single-zone dryer. This work recommends guidelines for choosing gas-flow rates, gas temperatures, and substrate thickness to minimize the residual solvent. The model predictions show that, at any gas temperature, the residual solvent is minimum at an intermediate gas-flow rate. The *trapping skinning* effect is less evident in thicker coatings and substrates.
 J Appl Polym Sci 87: 477–486, 2003

Key words: coatings; glass transition; thin films,

INTRODUCTION

Coated products such as audiotapes, videotapes, adhesives, and photographic films are produced in industrial dryers by drying polymer solutions that are cast onto a substrate. Drying is accomplished by vigorous impingement of hot drying gas on the polymer coatings. The drying gas temperature, flow rate, and humidity form three important operating conditions of any industrial dryer. Improper choice of the operating conditions can result in defects such as delamination, cracking, and starry night (a defect that can occur during drying of a polymer coating). The defect is a series of holes 1–100 microns in size. Because the holes appear like stars in the night against a black photographic film background, this defect is called starry night, that is, there are bubbles in the coating. Also, due to inappropriate choice of the operating conditions, the coatings may not meet residual solvent specifications due to anomalous *trapping skinning* behavior. Drying models help choose appropriate operating conditions for industrial dryers to produce defect-free coatings that meet residual solvent specifications.

Correspondence to: M. Vinjamur, Department of Chemical Engineering and Material Science, University of Minnesota, 151 Amundson Hall, 421-Washington Ave. SE, Minneapolis, MN 55455.

Contract grant sponsors: 3M; Avery-Dennison.

Journal of Applied Polymer Science, Vol. 87, 477–486 (2003)

Most of the earlier studies on drying models show the efficacy of models in predicting the drying behavior of polymer coatings. Okazaki et al.[1] utilized a drying model to delineate the drying mechanism of coatings that shrink during drying. Blandin et al.[2] used a one-dimensional model to describe the drying of paints to obtain the weight loss of the coating and solvent concentration profiles with time. Yapel[3] developed a detailed coupled heat-and-mass-transfer finite element model for the drying of coatings. Yapel[3] showed that most of the drying occurs during the initial stages, and due to a precipitous fall in the diffusion coefficient at low solvent concentrations, solvent removal becomes very slow in the later stages of drying. Vrentas and Vrentas[4] developed a set of equations to describe simultaneous mass and heat transfer during drying and suggested a solution scheme to solve the model. The authors claimed that the proposed model can be used to design the size of the dryer to reduce the solvent concentration to a desired level. Gutoff[5] developed an easy spreadsheet method that can be used to compute drying rates in nearly constant-rate and falling-rate periods. Saure et al.[6] modeled the drying of poly(vinyl acetate)/methanol solutions and claimed that the model predicts the drying time and is capable of estimating diffusion coefficients from the drying experiments. Price et al.[7] used a drying model to extract the diffusion parameters of Vrentas and Duda's[8] free-volume theory from gravimetric experiments by nonlinear regression. The above models do not explicitly show the effect of the operating conditions on the drying behavior.

There are, however, few works that describe the drying behavior at various operating conditions. Cairncross[9] modeled single-zone and multiple-zone dryers with infrared heating and developed guidelines for dryer design to produce coatings that meet residual solvent specifications without boiling during drying. Alsoy and Duda[10] used a model proposed by Vrentas and Vrentas[4] and showed that, for a poly(vinyl acetate)/toluene system, the time to dry to a 1% residual solvent does not depend on the drying gas-flow rates at high heat and-mass transfer coefficients because the drying rate is controlled by diffusion in the coating at high drying gas-flow rates. Alsoy and Duda[10] demonstrated that increasing the drying gas temperature drastically reduces the drying time to dry to a 1% residual solvent for a poly(vinyl acetate)/toluene system. Alsoy and Duda[11] modeled the multicomponent drying of polymer films and demonstrated the effect of the operating conditions on the residual solvent content. One of the features of the multi-component model, shown by the authors, is the ability to control the removal of individual solvents by changing the solvent composition in the gas phase.

All the models described above use Fick's law of diffusion with a concentration-dependent diffusion coefficient to describe the drying process. Some polymer solutions, however, are shown to exhibit non-Fickian behavior during sorption and can show similar behavior during drying. Non-Fickian behavior needs to be incorporated into the solvent mass conservation equation to describe the drying process completely from a mechanistic standpoint. This article shows and compares the effect of the operating conditions on the residual solvent content predicted by non-Fickian and Fickian models.

Durning and Tabor[12] developed a nonequilibrium thermodynamic theory to describe the solvent mass flux for non-Fickian models. During drying, stress develops due to shrinkage of the coating. The stress gradients contribute to solvent mass transport in addition to the solvent concentration gradients. The stress contribution increases due to a decrease in the solvent concentration and decays with the relaxation time, which depends on the temperature and the solvent concentration. We refer to the solvent transport due to stress gradients as *non-Fickian transport.*

During drying, some polymer coatings exhibit trapping skinning (Vinjamur and Cairncross[13]), where *more* solvent is trapped inside the coating dried at a *higher* drying gas-flow rate and/or temperature. Trapping skinning behavior is anomalous because Fick's law of diffusion cannot predict it.[14] Cairncross and Durning[15] investigated trapping skinning by a one-dimensional isothermal model for the drying of viscoelastic coatings utilizing the theory developed by Durning and Tabor.[12] Cairncross and Durning[15] described the diffusion coefficients and the relaxation times with exponential functions and proposed an indirect argument that increasing the drying gas temperature can produce a thicker coating after a fixed drying time. Edwards[16] employed a stepwise diffusion coefficient and relaxation time in an isothermal model and showed that trapping skinning occurs at higher mass-transfer coefficients (higher drying gas-flow rates). We utilized Vrentas and Duda's[8] free-volume theory, in a non-Fickian nonisothermal drying model, to describe diffusion coefficients and relaxation times. We demonstrated that trapping skinning occurs at higher drying gas-flow rates and recommend intermediate flow rates for drying of the polymer coatings to minimize residual solvent.

This article describes the effect of the drying gas temperature and flow rate on the residual solvent content. In an industrial dryer, the coating is heated from both the top and bottom surfaces, while evaporation takes place only from the top surface of the coating. So, this article discusses the effect of the top and bottom-surface flow rates on the residual solvent content. Also, this article elucidates the effect of the coating and substrate thickness on the trapping skinning behavior, which is known to occur at high drying gas-flow rates.

REVIEW OF NON-FICKIAN MODEL

Vinjamur and Cairncross[17] developed a coupled mass and heat-transfer model to describe drying of the coating and proposed a solution scheme to solve the equations. Vinjamur and Cairncross[17] obtained good qualitative agreement between experimentally measured trapping skinning results and those obtained from model predictions. We used the same model and present the final equation set in this article.

Mass conservation equation

The solvent mass conservation equation includes the transport due to the stress gradients:

$$\frac{\partial C}{\partial t} = \frac{\partial j}{\partial \xi} = \frac{\partial}{\partial \xi}\left(D\frac{\partial C}{\partial \xi}\right) + \frac{\partial}{\partial \xi}\left(E\frac{\partial \pi}{\partial \xi}\right) \tag{1}$$

C is the solvent concentration; π, the in-plane stress; t, the time, and ξ, the distance in the polymer material coordinates.[18] D is the mutual diffusion coefficient, and E, the diffusion coefficient that couples with the stress gradient. We used Vrentas and Duda's[8] free-volume theory to describe D, and E depends on D and the shear modulus of the polymer, G_0:

$$E = D\frac{\hat{V}_S^2 M_{WS} G_0}{RT}\frac{1}{(1 + C\hat{V}_S)[\partial(fC)/\partial C]} \tag{2}$$

TABLE I
Acetone and PMMA Parameters for the Model

Solvent parameters	Acetone	Polymer parameters	PMMA
D_0 (cm^2/s)	3.6×10^{-4}	K_{21}/γ (cm^3/g^{-1} K^{-1})	3.05×10^{-4}
K_{11}/γ (cm^3/g^{-1}K^{-1})	1.86×10^{-3}	$K_{22} - T_{g2}$ (K)	-301
$K_{21} - T_{g1}$ (K)	-53.33	$\hat{V}_2^*$ (cm^3)	0.788
$\hat{V}_1^*$ (cm^3)	0.943	τ_0 (s)	140
χ	0.4		
ξ	0.375		

V_S is the specific volume of the solvent; M_{WS}, the molecular weight of the solvent; R, the gas constant; and T, the temperature. f(C) is the fugacity of the solution and is a function of the activity of the solution. If the Flory–Huggins theory is used to describe the activity, then

$$E = D\frac{\hat{V}_S^2 M_{WS} G_0}{RT}\frac{C_S(1 + C_S\hat{V}_S)^2}{[1 + (1 - 2\chi)C_S\hat{V}_S]} \quad (3)$$

At the coating surface, the solvent flux, j, is described by a mass-transfer coefficient:

$$j = KP_{sat}(a^+ - a^\infty) \quad (4)$$

K is the mass-transfer coefficient; P_{sat}, the vapor pressure of the solvent at the coating temperature; a^+, the activity at the coating surface on the gas side; and a^∞, the activity in the bulk gas. At the coating substrate boundary, the solvent flux is zero:

$$j = 0 \quad (5)$$

Equations (4) and (5) represent two boundary conditions, and the uniform initial concentration is the initial condition for eq. (1).

Stress evolution equation

Maxwell's model with a single relaxation time describes the stress evolution during drying. At any point in the coating, the stress develops due to a change in the solvent concentration and decays with a relaxation time, τ_{relax}, which depends on the solvent concentration and the coating temperature:

$$g(C)\frac{dC}{dt} = \frac{d\pi}{dt} + \frac{\pi}{\tau_{relax}} \quad (6)$$

$g(C)$ is the ratio of the shear modulus of the polymer solvent mixture to that of the pure polymer.

Energy conservation equation

Since polymer coatings are thin, the temperature can be assumed to be uniform[4] across the coating thickness and a one-dimensional lumped equation describes the coating temperature evolution:

$$(m_1C_{p,1}l_1 + m_2C_{p,2}l_2 + m_3C_{p,3}l_3)\left(\frac{dT_c}{dt}\right) = (h_{top} + h_{bot})(T_{gas} - T_c) - \Delta H_v\dot{m} \quad (7)$$

m is the mass; and $C_{p,1}$, $C_{p,2}$, and $C_{p,3}$, specific heats of the solvent, the polymer, and the substrate, respectively, and are assumed to be constant. l is the thickness and subscripts 1, 2, and 3 stand for the solvent, the polymer, and the substrate, respectively. The first term on the left-hand side of eq. (7) is the effective specific heat of the coating; h_{top} and h_{bot}, top (gas)-side and bottom (substrate)-side heat-transfer coefficients; T_{gas}, the drying gas temperature; and T_c, the coating temperature. The product of the first two terms on the right-hand side of eq. (7) is the heat-transfer rate from the drying gas to the coating. ΔH_v is the latent heat of vaporization of the solvent; and $\dot{m}$, the rate of solvent evaporation; j, from the coating surface. The last term on the right-hand side represents heat consumption because of evaporative cooling.

The polymer is nonvolatile and its contribution to the total coating thickness does not change during drying. The contribution of the solvent thickness to the total coating thickness is obtained by integrating the solvent concentration through the dry film thickness, l_p:

$$l_s = \int_0^{l_p} C\hat{V}_s d\xi \quad (8)$$

RESULTS AND DISCUSSION

We chose poly(methyl methacrylate)/acetone (PMMA/Ac) solutions because Vinjamur and Cairncross[13] showed that these solutions are likely to exhibit non-

TABLE II
Physical Properties of Acetone and PMMA and Operating Parameters for the Non-Fickian Drying Model

Properties	Measurement
Acetone	
Specific volume (cm^3/g)	1.22
Specific heat (cal g^{-1} °C^{-1})	0.52
Latent heat of vaporization (cal/g)	125.11
ΔCp (cal g^{-1} °C^{-1})	0.4
T_g (K)	50
PMMA	
Specific volume (cm^3/g)	0.8417
Specific heat (cal g^{-1} °C^{-1})	0.30
G_0 (dynes/cm^2)	1.35×10^{10}
ΔCp (cal g^{-1} °C^{-1})	0.33
T_g (K)	381.0
Operating parameters and substrates	
Initial temperature (K)	298.0
Initial Ac concentration (w/w)	85%
Specific heat (cal g^{-1} °C^{-1})	0.45
Specific volume (cm^3/g)	0.725
Thickness (cm)	3.556×10^{-2}

Fickian behavior. Tables I and II list all the parameters required to solve the model equations except the operating parameters such as the drying gas temperature, heat-transfer and mass-transfer coefficients, and thickness of the coating. Heat-transfer coefficients that are typical of industrial dryers were chosen and mass-transfer coefficients were computed from the corresponding heat-transfer coefficients using the Chilton–Colburn analogy.

Drying of the polymer coatings is characterized by three periods, namely, warm-up, nearly constant-rate, and falling-rate periods. Figure 1 displays the three drying periods and shows the coating temperature and residual solvent content for a 100-micron dry polymer thickness PMMA/Ac coating at a drying gas temperature of 353 K and a heat-transfer coefficient of 5×10^{-3} (cal s^{-1} cm^{-2} K^{-1}). The cartoons in Figure 2 present key features of the drying behavior exhibited by drying coatings in the three periods. The arrows in Figure 2 indicate the direction of flux. NFF and FF stand for non-Fickian flux, $E(d\pi/d\xi)$, and Fickian flux, $D(dC/d\xi)$, respectively. Vinjamur and Cairncross[17] discussed the key features in detail, and it is pertinent to present them briefly here because they form the basis of the arguments and the explanations in this article.

In the warm-up period, the coating temperature increases or decreases rapidly due to initial transients

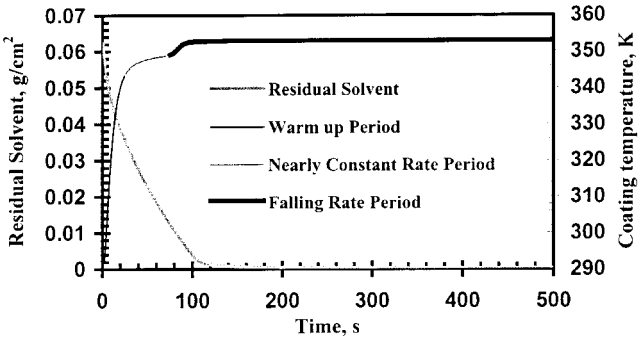

Figure 1 Coating temperature and the residual solvent for a 100-micron dry polymer thickness PMMA/Ac coating that is dried at a drying gas temperature of 353 K and a top- and bottom-surface heat-transfer coefficient of 5×10^{-3} cal s^{-1} cm^{-2} K^{-1}.

and an imbalance of heat transfer between the drying gas and the coating. A solvent concentration profile develops a sigmoidal shape that is flat at the coating

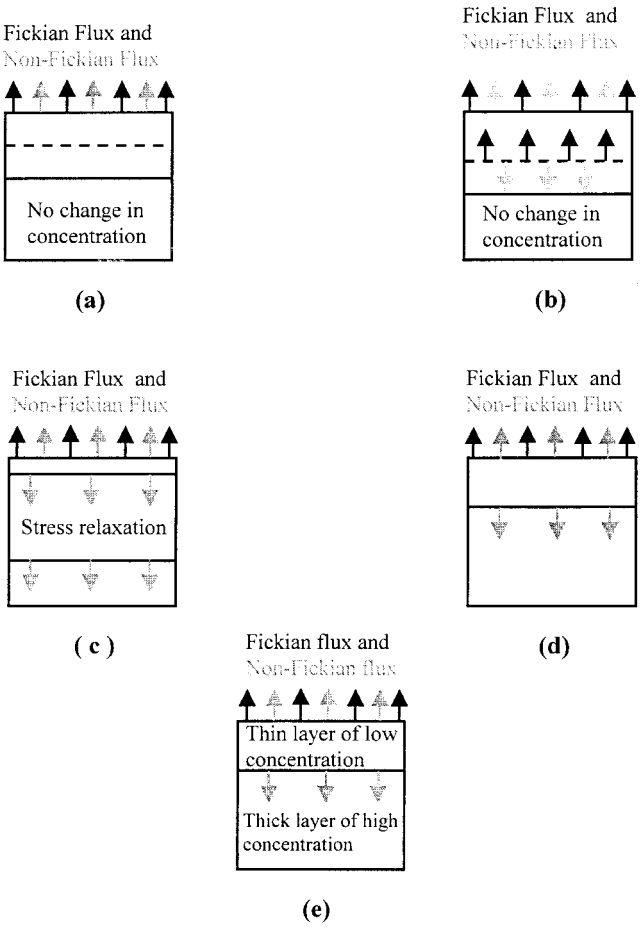

Figure 2 Schematic that demonstrates the drying behavior in the warm-up period [cartoons (a, b)] in the nearly constant-rate period [cartoons (c, d)] and in the falling-rate period [cartoon (e)]. Gray and black arrows indicate non-Fickian flux and Fickian flux, respectively. The dotted and the solid lines indicate the peak in Fickian flux and the concentration front, respectively.

surface and at the substrate and steep inside the coating. The flat solvent concentration gradient at the coating surface is due to the NFF at the coating surface that develops due to the stress gradient. The NFF draws more solvent to the coating surface from inside the coating. The solvent concentration gradient becomes steep inside the coating in response to a high total flux (NFF + FF) near the coating surface. The steep concentration gradient or front results in a peak in the FF, shown by dotted lines in Figure 2(a). As the coating dries, the peak in the FF, shown in Figure 2(b), and the concentration front move into the coating. Near the substrate, the concentration profile is flat in a region where the concentration does not decrease from its initial value. Also, in the warm-up period, due to high solvent concentrations and increasing coating temperature, relaxation times are short and the stress relaxes inside the coating. Relaxation causes a shoulder in the stress profile and a negative peak in the NFF.

In the nearly constant-rate period, the coating temperature remains nearly constant because the heat supplied by the hot drying gas is balanced by heat consumption due to evaporative cooling. In this period, due to nearly constant and high coating temperatures at high drying gas-flow rates, the stress does not develop significantly at the coating surface because of low relaxation times. Deeper in the coating, the stress relaxes and causes the NFF to vanish. Also, the NFF becomes negative deeper into the coating, shown in Figure 2(c), again due to stress relaxation. During the end of this period, D is low near the coating surface due to low solvent concentrations. Equation (3) shows that E becomes very low because of low D and solvent concentrations. During the end of this period, due to stress relaxation, the NFF becomes negative and results in a second solvent concentration front near the coating surface, shown in Figure 2(d).

In the falling-rate period, the coating temperature increases and reaches the drying gas temperature and the drying rate decreases because of a drastic drop in the solvent activity at a higher polymer concentration at the coating surface. The drying behavior of the polymer coatings (solvent concentration and stress profiles) does not change qualitatively in the falling-rate period because of a very low drying rate. The solvent concentration through the coating is low in this period and decreases very slowly due to low diffusion coefficients. Hence, the stress increases very slowly and does not relax anywhere in the coating due to high relaxation times at low solvent concentrations. Therefore, the stress profile maintains its shape in this period. The negative NFF that occurs during the end of the nearly constant-rate period remains negative. This negative NFF hinders the solvent transport and results in a steep solvent concentration gradient inside the coating. This leads to development of thin layer of a low solvent concentration near the coating surface and a thick layer of a high solvent concentration inside the coating, as shown in Figure 2(e). At higher gas-flow rates, the non-Fickian flux becomes negative closer to the surface and, therefore, results in a thinner layer of a low solvent concentration and a thicker layer of a high solvent concentration inside the coating. Thus, more solvent remains inside a coating dried at higher gas-flow rates and trapping skinning occurs. Vinjamur and Cairncross[13] experimentally measured trapping skinning for poly(methyl methacrylate)/acetone coatings at higher gas-flow rates.

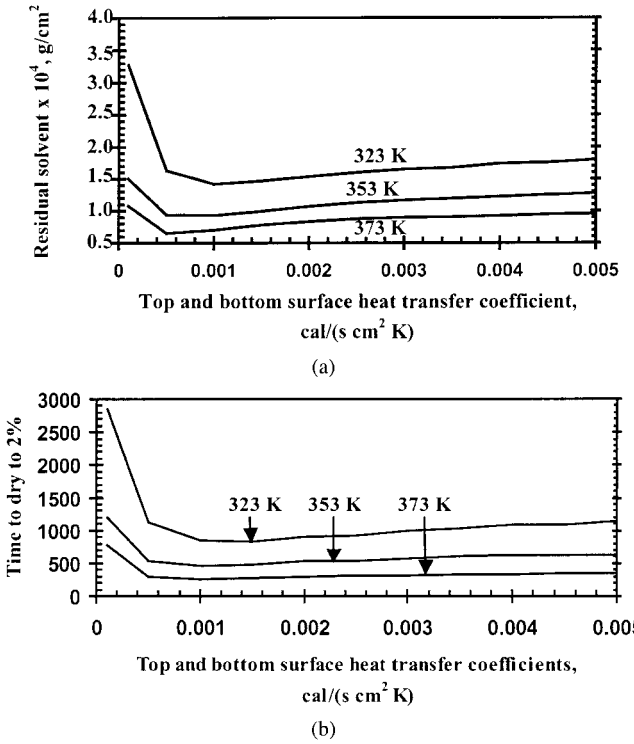

Figure 3 (a) Residual solvent at 2000 s versus heat-transfer coefficient for a 100-micron dry film-thickness PMMA/Ac coating at drying at temperatures of 323, 353, and 373 K. The residual solvent exhibits a minimum at an intermediate heat-transfer coefficient for all the three temperatures. (b) Time needed to dry a 100-micron dry film-thickness PMMA/Ac coating to 2% versus heat-transfer coefficient and at drying gas temperatures of 323, 353, and 373 K. The time exhibits a minimum at intermediate drying gas-flow rates for all the three temperatures.

Effect of drying gas-flow rate

Figure 3(a) shows the effect of the drying gas-flow rate on the residual solvent at three different air temperatures for a drying time of 2000 s for a 100-micron dry film thickness PMMA/Ac coating. Table III gives a list of heat-transfer and mass-transfer coefficients at different drying gas-flow rates. Heat-transfer coefficients typical of industrial dryers are chosen and mass-transfer coefficients are computed from the corresponding

TABLE III
Heat-transfer Coefficients (HTCs; cal s^{-1} cm^{-2} K^{-1}) and Mass-transfer Coefficients (MTCs; g s^{-1} cm^{-2} $mmHg^{-1}$) Computed from Chilton–Colburn Analogy and Residual Solvent Content (RSC; g/cm^2) Predicted by non-Fickian Model at 323, 353, and 373 K

	HTC × 10^3										
	0.1	0.5	1.0	1.5	2.0	2.5	3.0	3.5	4.0	4.5	5.0
	MTC × 10^3										
RSC	0.25	1.24	2.48	3.72	4.96	6.20	7.44	8.68	9.92	11.16	12.4
RSC × 10^4 at 323 K	3.27	1.64	**1.42**	1.47	1.54	1.60	1.65	1.68	1.74	1.76	1.80
RSC × 10^4 at 353 K	1.50	**0.94**	**0.93**	0.99	1.07	1.13	1.17	1.19	1.23	1.25	1.28
RSC × 10^4 at 373 K	1.08	**0.65**	0.70	0.78	0.83	0.88	0.90	0.91	0.92	0.95	0.96

heat-transfer coefficients using the Chilton–Colburn analogy. The residual solvent exhibits a minimum indicated by boldface in Table III, at all the three drying gas temperatures. The increase (from minimum at an intermediate heat-transfer coefficient to maximum at a high heat-transfer coefficient) in the residual solvent of about 23% at 323 K and 48% at 373 K is trapping skinning behavior of the coatings. At higher heat-transfer coefficients, the coating temperature increases faster than does the drying gas temperature and the stress relaxes closer to the coating surface than it does at lower heat-transfer coefficients. Therefore, the NFF becomes and stays negative closer to the surface at higher heat-transfer coefficients. This causes development of a thinner region of low solvent concentration near the coating surface and a thicker region of high solvent concentration deeper within the coating, at higher heat-transfer coefficients or drying gas-flow rates. So, *more* solvent remains in the coating dried at higher gas-flow rates.

Figure 3(a) shows that at higher drying gas temperatures the minimum in the residual solvent occurs at lower heat-transfer coefficients (i.e., at lower drying gas-flow rates). The heat-transfer rate from the hot drying gas to the coating depends directly on the heat-transfer coefficient and the temperature difference between the drying gas and the coating. The coating temperature increases faster at higher drying gas temperatures due to higher heat-transfer rates. Consequently, due to high coating temperatures, the stress relaxes and results in the negative NFF closer to the coating surface at low gas-flow rates and high gas temperatures. The negative NFF causes a steep solvent concentration gradient and leads to development of a thinner region of low solvent concentration and a thicker region of high solvent concentration at lower drying gas-flow rates at higher gas temperatures. On the other hand, at lower drying gas temperatures, in the falling-rate period, the negative NFF occurs closer to the coating surface at higher gas-flow rates. Hence, the region of low solvent concentration is thinner at the coating surface and the region of high solvent concentration is thicker inside the coating at higher drying gas-flow rates at lower gas temperatures.

Figure 3(b) shows the time needed to dry coatings to a 2% residual solvent for a 100-micron dry film thickness of the PMMA/Ac coating at three different drying gas temperatures. At higher drying gas-flow rates at all the three drying gas temperatures, the stress relaxation occurs closer to the coating surface. As a consequence, the NFF becomes negative closer to the coating surface and hinders the solvent transport from inside the coating. So, it takes longer to dry to a 2% residual solvent content at higher drying gas-flow rates at all the three temperatures.

The above claim of using intermediate drying gas-flow rates needs to be tempered when some mechanical aspects of industrial dryers are considered. Aust et al.[19] stated that a certain minimum drying gas-flow rate or velocity is required to maintain the sinusoidal shape of the substrate in a flotation dryer. The drying gas-flow rates at which the minimum residual solvent occurs may be lower than the minimum flow rate needed in the flotation dryer. Therefore, the drying gas-flow rates that allow for the handling of the coating inside the dryer and also result in a lower residual solvent should be used in the dryers. Since heat-transfer coefficients vary as the square root of the drying gas velocity or flow rate, operating the dryer at intermediate drying gas-flow rates instead of higher gas-flow rates can reduce the operating costs of the dryer.

Effect of dry film thickness

Figure 4(a, b) show variation of the residual solvent with the heat-transfer coefficient for 150- and 200-micron dry film thicknesses, respectively. As discussed for results shown in Figure 3(a), the residual solvent exhibits a minimum with the gas-flow rate at both these thicknesses. Also, at higher drying gas-flow rates, the percentage increase in the residual solvent from the minimum decreases for the 200-micron dry

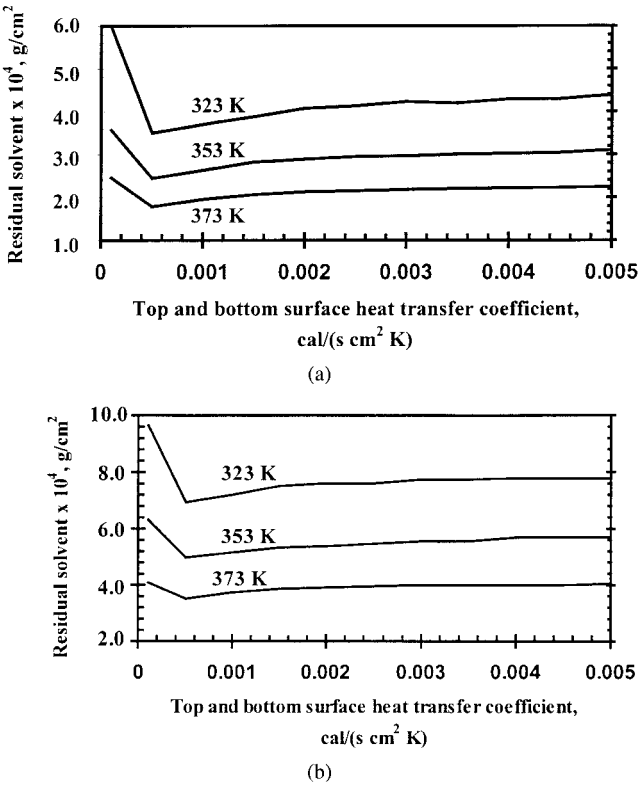

Figure 4 (a) Residual solvent at 2000 s versus heat-transfer coefficient (with equal top- and bottom-surface heat-transfer coefficients) for a 150-micron dry film-thickness PMMA/Ac coating at drying gas temperatures of 323, 353, and 373 K. The residual solvent exhibits a minimum at an intermediate heat-transfer coefficient for all the three temperatures. (b) Residual solvent at 2000 s versus heat-transfer coefficient (with equal top- and bottom-surface heat-transfer coefficients) for a 200-micron dry film-thickness PMMA/Ac coating at drying gas temperatures of 323, 353, and 373 K. The residual solvent exhibits a minimum at an intermediate heat-transfer coefficient for all the three temperatures.

film thickness coating. Even for thicker films, the region of low solvent concentration near the coating surface is thinner and the region of high solvent concentration deeper within the coating is thicker at higher gas-flow rates. But, as the dry film becomes thicker, the increase in the thickness of the region of high solvent concentration deeper in the coating, at higher gas-flow rates, becomes insignificant. Hence, the increase in the residual solvent at higher drying gas-flow rates decreases for thicker films. Extending this argument further, in very thick films, trapping skinning may not be observed.

Effect of drying gas temperature

Figures 3(a) and 4(a, b) show that the residual solvent decreases with an increase in the drying gas temperature. Although a thinner region of low solvent concentration near the coating surface and a thicker region of high solvent concentration inside the coating develop, the residual solvent does not exhibit a minimum with the drying gas temperature. Therefore, an increase in the drying gas temperature always results in a decrease in the residual solvent because the solvent levels are lower both in the thinner and thicker regions of the coating due to higher transport coefficients at higher gas temperatures.

Effect of non-Fickian transport

Non-Fickian transport occurs due to stress gradients in the direction of decreasing stress. The NFF describes the non-Fickian transport. The NFF anywhere in the coating is given by the product of E and the stress gradient. Equation (3) shows that E depends directly on the mutual diffusion coefficient, D, the elastic modulus, G_0, of the polymer, and the solvent concentration. So, the stress gradient and the solvent concentration at the coating surface in the three drying periods, the coating temperature, and the elastic modulus of the polymer determine the contribution of the NFF. The NFF can vanish if the stress gradient disappears or it can change its direction due to stress relaxation.

Figure 5 shows the residual solvent predicted by our non-Fickian model and the corresponding Fickian model. The Fickian model is solved separately and it describes solvent transport only due to the solvent concentration gradient and the stress is always zero at all points in the coating. The Fickian model is created by setting the diffusion coefficient in the non-Fickian term to zero and the relaxation time in the stress-evolution equation to 1×10^{-6}s (very fast relaxation). Figure 5 shows that, unlike the non-Fickian model, the Fickian model does not predict trapping skinning at higher drying gas-flow rates, that is, there is no increase in the residual solvent at higher drying gas-flow rates or heat-transfer coefficients at both these

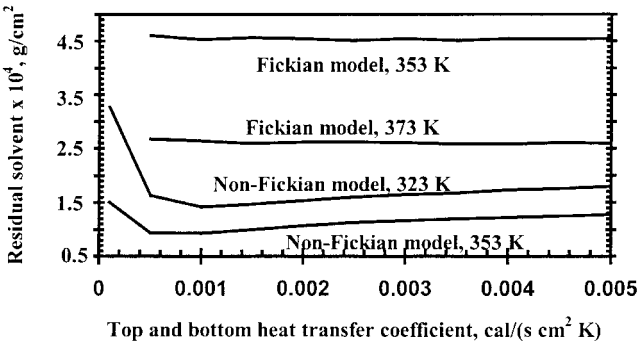

Figure 5 Residual solvent at 2000 s for a 100-micron dry film-thickness PMMA/Ac coating versus heat-transfer coefficient (with equal top-and bottom-surface heat-transfer coefficients) predicted by Fickian model at drying gas temperatures of 353 and 373 K and by non-Fickian model at gas temperatures of 323 K and 353 K. Non-Fickian model predicts lower residual solvent at lower gas temperatures than Fickian model at higher gas temperatures.

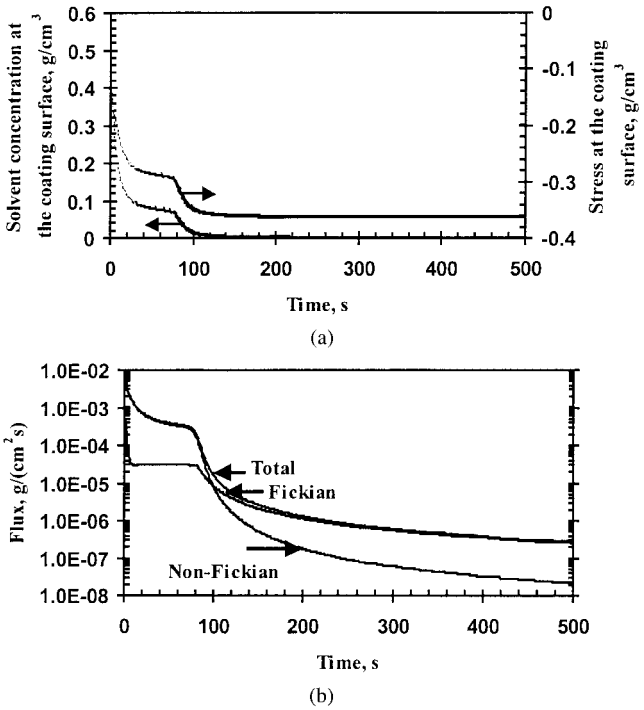

Figure 6 (a) Solvent concentration and stress evolution at the coating surface at a heat-transfer coefficient of 5×10^{-3} (cal s^{-1} cm^{-2} K^{-1}) and a drying gas temperature of 353 K for a 100-micron dry film-thickness PMMA/Ac coating, in the warm-up, nearly constant-rate, and falling-rate periods indicated by the dotted, serrated, and thick lines, respectively. (b) Fickian, non-Fickian, and total flux evolution at the coating surface at a heat-transfer coefficient of 5×10^{-3} (cal s^{-1} cm^{-2} K^{-1}) and a drying gas temperature of 353 K for a 100-micron dry film-thickness PMMA/Ac coating.

temperatures. As discussed above, the non-Fickian model does capture trapping skinning behavior at higher drying gas-flow rates.

Surprisingly, the non-Fickian model predicts a lower residual solvent at 323 K than that predicted by the Fickian model at 353 and 373 K for PMMA/Ac coatings. This is because the NFF that occurs due to stress gradients drives the solvent out of the coating in all the three drying periods. Figure 6(a) depicts the solvent concentration and the stress evolution at the coating surface, at a heat-transfer coefficient of 5×10^{-3} (cal s^{-1} cm^{-2} K^{-1}) and a drying gas temperature of 353 K for the 100-micron thickness PMMA/Ac coating. In the warm-up period, E is high at the surface, due to a high solvent concentration. In the nearly constant-rate period, E is high due to high D at high coating temperatures and significantly high solvent concentrations at the surface. In the falling-rate period, E is low due to low D and solvent concentration. The stress gradient at the surface is high in the warm-up and the nearly constant-rate period and diminishes in the falling-rate period. Therefore, Figure 6(b) shows that the NFF is high in the warm-up and the nearly constant-rate periods and low in the falling-rate period. So, the NFF always drives the solvent out of the coating and aids in faster solvent removal.

The result that the non-Fickian model predicts a lower residual solvent at lower drying gas temperatures suggests that the Fickian model gives conservative estimates of the residual solvent. Hence, an industrial dryer designed with the Fickian model may be operated at lower drying gas temperatures to meet the residual solvent specifications. Lowering the drying gas temperature can result in substantial energy savings and, therefore, can decrease the operating costs of the dryer.

Effect of top-surface and bottom-surface drying gas-flow rates

Typically, in industrial dryers, the coatings are heated from both the top and the bottom surfaces during drying. So, the transfer (mass and heat) coefficients on the top-and the bottom-coating surfaces can be varied independently by changing the respective drying gas-flow rates. This gives a control on the heat-transfer and mass-transfer rates that occur between the hot drying gas and the coating. Lower drying gas-flow rates result in lower transfer coefficients while higher transfer coefficients can be obtained at higher gas-flow rates.

Figure 7(a–c) show the residual solvent for different bottom-surface heat-transfer coefficients at drying gas temperatures of 323, 353, and 373 K for three different top-surface heat-transfer coefficients, namely, 1×10^{-4} (low), 2×10^{-3} (medium), and 5×10^{-3} (high) cal s^{-1} cm^{-2} K^{-1}. There is a minimum in the residual solvent only at the low top-surface heat-transfer coefficient. The effect of trapping skinning is seen only at high gas-flow rates. Therefore, at the low top-surface heat-transfer coefficient, the residual solvent decreases with increasing bottom gas-flow rates at low bottom-surface heat-transfer coefficients. As the bottom-surface heat-transfer coefficient is increased, trapping skinning occurs and more solvent is trapped in the coating. At medium- and high-top surface heat-transfer coefficients, the coating is heated sufficiently fast that trapping skinning occurs even at low bottom-surface heat-transfer coefficients. At lower drying gas temperatures, the residual solvent is minimum at the medium top-surface heat-transfer coefficient and the low bottom-side heat-transfer coefficient. With an increase in the drying gas temperature, the minimum in the residual solvent shifts to both the low top-surface and bottom-surface heat-transfer coefficients. The shift in the residual solvent is discussed in the effect of the drying gas-flow rate section. The above discussion on the effect of the top-surface and bottom-surface drying gas-flow rates has implications on the design of industrial dryers. The results in this section suggest that the dryer should be operated at medium drying gas-flow

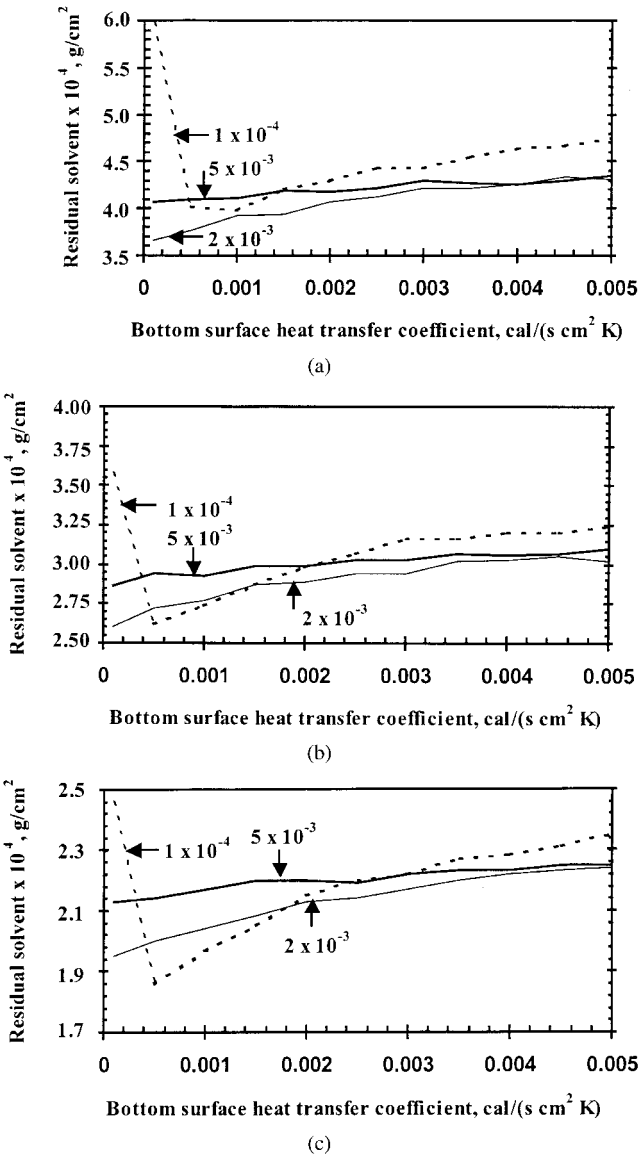

Figure 7 (a) Residual solvent at 2000 s versus bottom-surface heat-transfer coefficient for three different top-surface heat-transfer coefficients for a 100-micron dry film-thickness PMMA/Ac coating at a drying gas temperature of 323 K. (b) Residual solvent at 2000 s versus bottom-surface heat-transfer coefficient for three different top-surface heat-transfer coefficients for a 100-micron dry film-thickness PMMA/Ac coating at a drying gas temperature of 353 K. (c) Residual solvent at 2000 s versus bottom-surface heat-transfer coefficient for three different top-surface heat-transfer coefficients for a 100-micron dry film-thick PMMA/Ac coating at a drying gas temperature of 373 K.

rates on the top-coating surface and low gas-flow rates on the bottom surface.

In the state-of-the-art floatation dryers, however, the same drying gas-flow rates are maintained on both surfaces to keep the coating away from the nozzles of the dryer. Another aspect that needs to be considered in deciding the drying gas flow-rates is the risk of explosions in the dryers. At low drying gas-flow rates and high rates of evaporation, Aust et al.[19] reported that a lower explosion level can be exceeded in the dryers. Hence, in the light of mechanical stability to keep the coating in a sinusoidal shape and to avoid the risks of explosion, dryers may be operated at medium drying gas-flow rates in all the zones.

Effect of substrate thickness

The substrate thickness affects the heat-transfer rate from the drying gas to the substrate and, thus, the coating temperature evolution from the initial temperature to the drying gas temperature. The thicker the substrate, the slower is the heat-transfer rate and the slower is the increase in the coating temperature. The substrate thickness can affect the drying behavior significantly because the transport properties (D and E) and the relaxation time are a strong function of temperature. Since the substrate thickness can be altered easily, changing the thickness provides a good handle to control the drying behavior.

Figure 8 shows the residual solvent for two different substrates (0.3556 and 0.03556 cm) for a 100-micron dry film thickness of the PMMA/Ac coating for two drying gas temperatures. The thin and thick curves indicate thin and thick substrates, respectively. At 323 K, unlike the thin substrate, the residual solvent does not increase at a higher heat-transfer coefficient for the thick substrate. At 373 K, the increase in the residual solvent from a heat-transfer coefficient of 3×10^{-3} cal s^{-1} cm^{-2} K^{-1} to 5×10^{-3} cal s^{-1} cm^{-2} K^{-1} is marginal (about 1.5%). Therefore, trapping skinning does not occur or decreases with thicker substrates.

As discussed in the Effect of Dry Film Thickness section, more solvent remains in the coating or trapping skinning occurs at higher drying gas-flow rates because the NFF becomes and stays negative closer to the coating surface and a region of high solvent con-

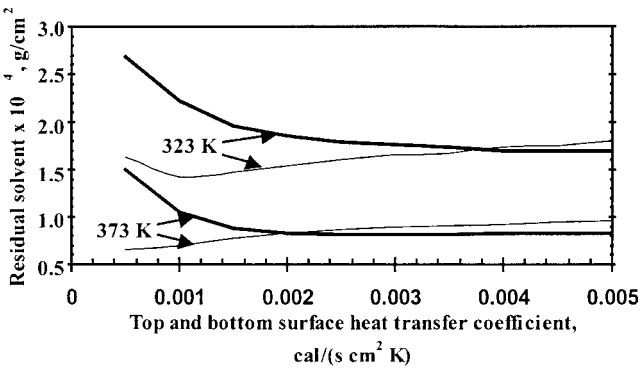

Figure 8 Residual solvent at 2000 s versus heat-transfer coefficient (with equal top- and bottom-surface heat-transfer coefficients) for a 100-micron dry film-thickness PMMA/Ac coating at drying gas temperatures of 323 and 373 K for two different substrate thicknesses. The thin and thick lines indicate thin and thick substrates, respectively.

centration develops inside the coating. With thicker substrates, the coating temperature increases more slowly. Hence, the stress relaxes and NFF becomes negative deeper into the coating because of shorter relaxation times at higher solvent concentrations. This results in a thinner region of high solvent concentration inside the coating. Therefore, residual solvent decreases or marginally increases at higher drying gas-flow rates.

CONCLUSIONS

The model presented in this article has a potential value for aiding in the design of industrial dryers, which involves choosing appropriate operating conditions such as the drying gas temperature and top- and bottom-surface gas-flow rates. It also reports the effect of operating conditions on the anomalous trapping skinning behavior of polymer coatings that occurs at higher drying gas-flow rates and/or temperatures. In selecting the proper operating conditions, the results should be evaluated from the standpoint of the mechanical stability of the coating and the risk of explosions in the dryers.

At higher drying gas-flow rates, the negative NFF that results due to the stress relaxation leads to a steep solvent concentration gradient inside the coating. This results in a thin region of low solvent concentration near the coating surface and a thick region of high solvent concentration inside the coating. At higher drying gas-flow rates, the coating temperature increases faster and the NFF becomes negative closer to the coating surface. Hence, the region of low solvent concentration becomes thinner and the region of high solvent concentration becomes thicker at higher drying gas-flow rates. This results in trapping skinning at higher drying gas-flow rates. The increase in the residual solvent is about 44% at 323 K and 46% at 373 K. The results of the effect of the top- and the bottom-surface drying gas flows suggest that medium gas-flow rates should be used on both surfaces to avoid trapping skinning.

Trapping skinning may not be observed with very thick dry films. Another interesting feature is that the non-Fickian model predicts faster solvent removal than does the Fickian model under the same operating conditions. Even when the drying gas temperature in the Fickian model is 50 K higher, the non-Fickian model predicts faster solvent removal. This is because the NFF always drives the solvent out of the coating at the surface.

The authors gratefully acknowledge the financial support of 3M and Avery-Dennison for this work.

References

1. Okazaki, M.; Shioda, K.; Masada, K.; Toei, R. J Chem Eng Jpn 1974, 7, 99.
2. Blandin, H. P.; David, J. C.; Vergnaud, J. M.; Illien, J. P.; Malizewicz, M. J Coat Technol 1987, 59, 27.
3. Yapel, R. A. Masters Thesis, University of Minnesota, Minneapolis, 1988.
4. Vrentas, J. S.; Vrentas, C. M. J Polym Sci Polym Phys 1994, 32, 187.
5. Gutoff, E. J Imag Sci Technol 1994, 38, 184.
6. Saure, R.; Wagner, G. R.; Schlunder, E. Surf Coat Technol 1998, 99, 253.
7. Price, E. P., Jr.; Wang, S.; Romdhane, I. H. AIChE J 1994, 43, 1925.
8. Vrentas, J. S.; Duda, J. L. J Polym Sci Polym Phys Ed 1977, 15, 403.
9. Cairncross, R. A. Ph.D. Thesis, University of Minnesota, Minneapolis, 1994.
10. Alsoy, S.; Duda, J. L. Dry Technol 1998, 16, 15.
11. Alsoy, S.; Duda, J. L. AIChE J 1999, 45, 896.
12. Durning, C. J.; Tabor, M. Macromolecules 1986, 19, 2220.
13. Vinjamur, M.; Cairncross, R. A. J Appl Polym Sci 2002, 83, 2269.
14. Crank, J. Trans Faraday Soc 1950, 46, 450.
15. Cairncross, R. A.; Durning, C. J. AIChE J 1996, 42, 2415.
16. Edwards, D. A. Chem Eng Commun 1998, 166, 201.
17. Vinjamur, M.; Cairncross, R. A. submitted for publication in AIChE J.
18. Billovits, G. F.; Durning, C. J. Chem Eng Commun 1989, 82, 21.
19. Aust, R.; Durst, F.; Raszillier, H. Chem Eng Proc 1997, 36, 496.